

Analysis and Design Methodology for System Cost Reduction in Distributed Power Systems

Wardah Inam, Thipok Rak-amnouykit and David J. Perreault
 Massachusetts Institute of Technology
 Cambridge, MA, US
 wardah@mit.edu, thipok16@mit.edu and djperrea@mit.edu

Khurram K. Afridi
 University of Colorado Boulder
 Boulder, Colorado, US
 khurram.afриди@colorado.edu

Abstract—This paper focuses on analyzing system-level cost and efficiency trade-offs in designing converters for power systems. We address the optimization of power converters to meet system-level goals of microgrids for rural electrification and propose a weighted efficiency criteria, derived from the percentages of energy processed by the converter at different power levels. We also propose a method to trade-off efficiency and cost of converters to decrease overall system cost and have developed two types of converters to demonstrate this proposed methodology.

I. DESIGNING CONVERTERS TO REDUCE SYSTEM COST

Power converters play a major role in determining the total system cost of many applications, such as distributed energy and electricity backup systems. However, detailed analysis of the impact of converter efficiency's variation with load on total system cost has rarely been discussed in literature. Several works have investigated the cost of individual components that affect the power converter cost [1], [2]. Significant progress has also been made on the optimization of reliability versus cost [3], [4]. While some works compare efficiency and cost of different system topologies [5], works that model and assess the total system cost impact of converters are still rare [6]. A sophisticated design methodology, which determines the cost and efficiency trade-off of power converters, will enable us to better evaluate new topologies and decrease the total system cost.

Power converters are usually designed to meet objectives such as optimizing efficiency or reducing converter cost, without considering the impact of the converter on overall system performance and cost. For high-efficiency applications, the design emphasizes on increasing the peak efficiency and/or a source-related weighted efficiency, such as the California Energy Commission "CEC" efficiency [7]. For low-cost applications, the design often emphasizes the cost of the converter, rather than the initial or the lifetime cost of the system. Hence, power converters with low component count are often utilized, minimizing the converter's cost, but not necessarily the system's initial or lifetime cost. The discrepancy between these two approaches arises because no framework exists to assess the design trade-off between efficiency and cost over the lifetime of an application. These design decisions have prevailed in part because there have been few opportunities to co-design the power converters and the entire application. However, in

creating new power systems (e.g. dedicated microgrids, power distribution systems, etc.), there is an opportunity to truly co-design and co-optimize the power system and the power converters.

In this paper, the optimization of converters to meet system-level goals is discussed. A weighted efficiency metric, derived from the percentage of energy processed by the converter at each power level and based on system-level studies, is proposed. The metric helps design power converters which will minimize the total energy loss in the system. This is followed by a method to evaluate the trade-off between efficiency and cost of power converters, aiming to decrease overall system cost. The trade-off helps justify the increased cost of the converter and identify the power converter that achieves the lowest system cost. We demonstrate this methodology using two types of load converters on a microgrid system for rural electrification. The methodology can also be extended to evaluate the source converter design for this microgrid system, or to other energy applications entirely.

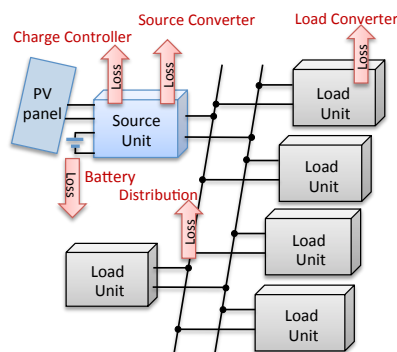


Figure 1: A system with six Power Management Units depicting the losses incurred

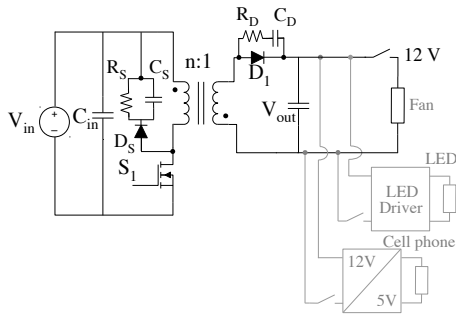
II. APPLICATION: AFFORDABLE ELECTRICITY ACCESS

The design methodology presented in this paper can be applied to a range of applications, especially those in which the power converter's cost of production or typical efficiency metrics do not completely represent the total cost of the system.

Globally, more than 1.2 billion people do not have access to electricity [8]. The cost of electricity infrastructure presents an economic obstacle to electrification of many impoverished communities. To develop solutions which can provide affordable access to electricity, we must aim to minimize the total system cost. In this paper, we consider the microgrid architecture proposed earlier [9], which consists of two Power Management Units (PMUs). The generator module interfaces with solar panels and batteries, and sets up the network voltage. The consumer module is a point-of-load converter, providing power conversion necessary to power different loads such as LED lights, cell phones, fans, etc. Fig. 1 shows a building block of the microgrid consisting of one generating unit and five consuming units. These building blocks can be repeated in different configurations to form an ad hoc microgrid.

III. CONVERTERS EVALUATED

Two types of load converters, hard-switched PWM and soft-switched resonant, were built to demonstrate the proposed methodology. For the hard-switched converter, the flyback topology was selected. The soft-switched resonant converters had two different design variations: first version incorporated a transformer with litz wire winding and second version incorporated a transformer with printed circuit board winding.



(a) Schematic of the flyback converter



(b) Prototype of the flyback converter

Figure 2: Flyback converter

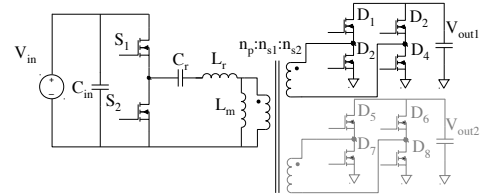
A. Flyback Converter

Flyback converter is one of the simplest and most-common power conversion topologies for low-power isolated conver-

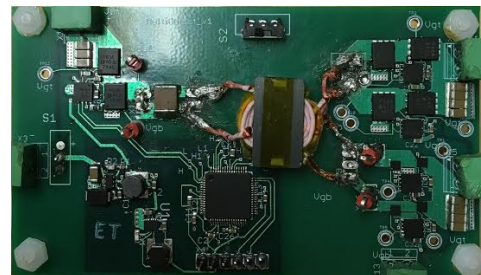
Table I: Components of the 12 V main power stage of the flyback converter

Component	Type	Cost(\$)
Inverters		
Input Capacitors	10 μ F/50V Ceramic capacitors, Qty: 5	0.068
Transistors	150V/26A MOSFET (FDD390N15A), Qty:1	0.472
	3.3k Ω (2W) Resistor Qty:1	
Snubber	22nF/100V Capacitor, Qty:1	0.155
	100V/1A Schottky diode, Qty: 1	
Control IC	Current-mode flyback dc/dc controller (LTC3805), Qty: 1	1.760
Transformer Rectifier		
	Power transformer (FA2900) Qty:1	1.890
Diode	60V/3A Schottky diode (PMEG6030), Qty:1	0.120
	33 Ω (1W) Resistor, Qty:1	
Diode Snubber	240pF/100V NPO Capacitor, Qty:1	0.047
Output Capacitor	22 μ F/16V Ceramic capacitors	0.054
Protection		
Switch	20V/4.2A MOSFET (SMD15PL), Qty: 1	0.054
Fuse	Fuse Glass 2AG, Qty: 1	0.180
	250V/10A Clip cartridge	
Output Diode	30V/2A Schottky diode, Qty: 1	0.045

sion. It requires very few components; a simple flyback power stage consists of a switch, a transformer and a diode. Despite the advantage of simplicity, there are some drawbacks: the converter suffers high device stresses, requires a gapped energy storage transformer, and is relatively large in volume. The schematic and prototype board of the flyback converter built are shown in Fig. 2. The flyback main power stage is followed by dedicated post-regulators to manage powering of cell-phones and LEDs. In this analysis only the 12 V main power stage will be considered. The components used for the power stage of the converter are detailed in Table I, and the cost of the power stage is provided in Fig. 5.

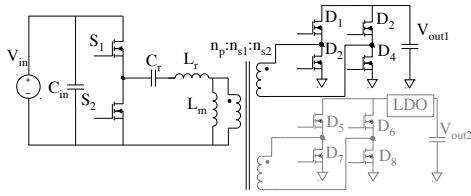


(a) Schematic of the first version of the resonant converter

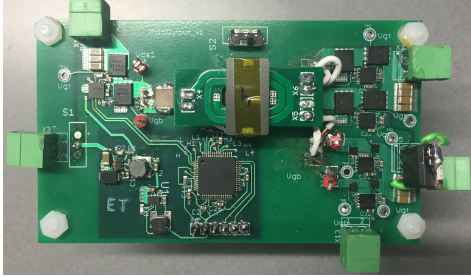


(b) Prototype of the first version of the resonant converter

Figure 3: Multi-output resonant converter with litz wire transformer



(a) Schematic of the second version of the resonant converter



(b) Prototype of the second version of the resonant converter

Figure 4: Multi-output resonant converter with PCB transformer

B. Multi-output Resonant Converter

Two variations of an LLC resonant converter, as shown in Fig. 3 and Fig. 4, have been developed with the goal of directly supplying both 12V and 5V outputs at high efficiency. The switching frequency gives us control over the voltage levels of both outputs, while the phase shift on the synchronous rectifier allows us to adjust individual outputs. Due to cross-regulation, both frequency control and phase shifting are necessary for an effective output voltage control.

The first version of the resonant converter utilizes a transformer with litz wire winding, while the second version utilizes a transformer with printed circuit board winding. The two outputs of these converters are V_{out1} (12 V) and V_{out2} (5 V), thus requiring a minimum transformer turns ratio of 12:12:5 if the voltage conversion is provided by only the transformer. An efficient design of the transformer can be challenging if large numbers of turns are used to realize an exact turns ratio, leading to higher copper requirement. Hence, for these transformers, we select a turns ratio of 2:2:1, with phase shift control to step the output voltage down from 6 V to 5 V in the first variation (Fig. 3a) and with an LDO post regulator to step down the voltage in the second variation (Fig. 4a). The transformer leakage inductance acts as the resonant inductor (L_r). This leakage inductance was estimated using the transformer's cantilever model [10].

1) First version - Transformer with litz wire winding:

Table II details the components used in the 12 V power stage of prototype converter. The cost of the main power stage is summarized in Fig. 5 which also includes cost of the protection devices detailed in Table I. The transformer is composed of an EELP18 core of N49 material with a gap resulting in a magnetizing inductance of $4.87 \mu\text{H}$. The primary winding is 4 turns of 48 AWG/450 strands litz wire. The secondary wind-

Table II: Components of the 12 V power stage of the resonant converters

Component	Type	Cost(\$)
Inverter		
Input Capacitors	10 μF /50V Ceramic capacitors, Qty: 4	0.068
Gate Drivers	120V/3A High and low side driver (UCC27201D), Qty: 1	1.310
Transistors	40V/21A TrenchFET (SIR836DP), Qty: 2	0.248
Transformation		
Capacitor	0.1 μF /50V Ceramic COG capacitor Qty: 2	0.119
Transformer (Litz wire)	EELP 18, N49 core Primary: 4 turn, 48 AWG/450 strands litz wire Secondary 1: 4 turn, 48 AWG/450 strands Secondary 2: 2 turn, 48 AWG/450 Strands	4.500
Transformer (PCB)	EILP 18, N49 core with clamp and 4 oz copper PCB Primary and Secondary 1: 4 turns Secondary 2: 2 turns	0.708
Rectification		
Mosfets	20V/20A TrenchFET (SIR484DP), Qty:4	0.302
Gate Drivers	100V/1.2A Half bridge gate driver, Qty: 2	1.582
	Bootstrap capacitor: 0.1 μF /50V	0.007
	Bypass capacitor: 10 μF /25V	0.067
Digital Isolator	150Mbps 2.5kV/ μs Dual channel isolator, Qty:1	0.833
Output Capacitors	10 μF /50V Ceramic capacitors, Qty: 4	0.095

Table III: Summary of transformer parameter measurements for cantilever model

Parameter	Approximate Measured Value (Litz wire Transformer)	Approximate Measured Value (PCB Transformer)
L_{11}	4.87 μH	3.35 μH
l_{12}	200 nH	100 nH
l_{13}	11.37 μH	726 nH
l_{23}	465 nH	358 nH
n_2	1	1
n_3	0.5	0.5

ings for 12 V and 5 V outputs are 4 and 2 turns of the same litz wire, respectively. Because the transformer was not fully packed, the copper loss can be reduced in the future design iteration. The effective leakage inductance (L_r) was around 200 nH. The summary of measured transformer parameters is provided in Table III. Agilent's 4395A impedance analyzer, Tektronix MSO4104 Oscilloscope and P6139a voltage probes were used for these measurements. A capacitance (C_r) of 200 nF was used and the converter operates, almost at resonance, at 800 kHz.

Phase shift between the bridge legs of the rectifier was implemented to drop the voltage from 6 V to 5 V, at the second output. The control signal for the 12 V full-bridge rectifier is in phase with the control signal for the inverter bridge. One of the legs of the 5V rectifier is in phase with the inverter bridge, while the second leg is phase-shifted to decrease the output voltage. The phase shift was decreased from 12.3% to 1.8% with increase in load.

2) *Second version - Transformer with PCB winding:* To reduce cost from the previous litz wire version, the transformer winding was instead printed on a 4 oz copper, 6 layer circuit

board. The cost of using 4 oz copper is slightly higher compared to that of 1 oz copper, but 4 oz copper yields higher efficiency. The increased cost per board has been taken into account as the increased transformer cost in Table II. For this prototype, phase-shift control was not very effective because the leakage inductance L_{13} of the PCB windings (as presented in the cantilever model) is very small. Hence, an LDO was added to decrease the output voltage from 6 V to 5 V. The transformer core is gapped to achieve a magnetizing inductance of $3.35 \mu\text{H}$. It had a leakage inductance of 150 nH, which acts as the resonant inductor (L_r), and a capacitance (C_r) of 200 nF. This converter operates around 915 kHz.

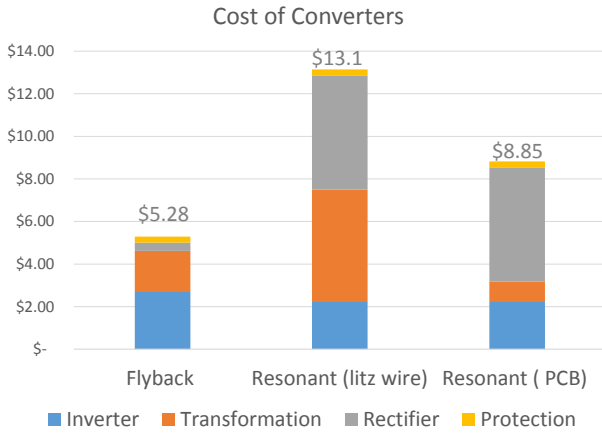


Figure 5: Cost of the 12 V power stage of the three converters

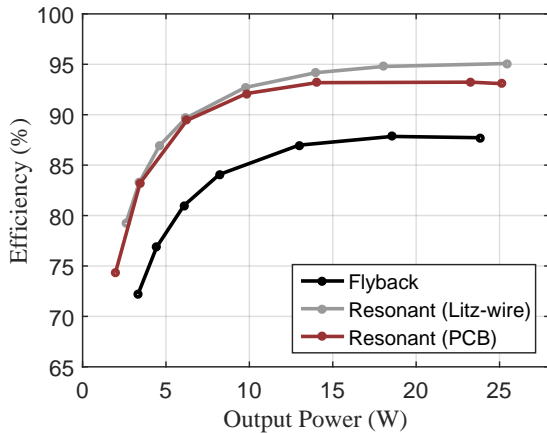


Figure 6: Efficiency vs output power of the three converters

IV. DETERMINING THE CONVERTER'S WEIGHTED EFFICIENCY METRIC THAT MINIMIZES ENERGY LOSS

In this section, we propose a weighted efficiency metric, which is derived from the load profile and based on the actual percentage of energy processed by the converter at each power level during a year. To determine the converter's efficiency profile that would result in minimum energy loss,

we first calculate the annual load profile of the converter from several system characteristics and the usage model. From the load profile, the fraction of time in a year that the load converter spends at each output power level is computed, then the fraction of output energy drawn at each power level is calculated. Combining this histogram with the efficiency versus output power curve, the weighted efficiency of each converter can be determined.

A. Annual Load Profile

The estimation of the annual load profile takes into account the loads, the variation of each load's power consumption, and the duration each load will be used in a year. Our microgrid system for rural electrification consists of four load types - an indoor light bulb (3 W), an outdoor light bulb (3 W), a fan (15 W), and a cell phone (2.5 W). Each load's power consumption is modelled considering product and manufacturing variations. Because the annual usage data does not exist for this newly created power system, it is necessary to construct a usage model and determine usage duration of each load. The model also incorporates user behavioral information collected from interviews, along with relevant physical data of the system location, such as irradiance and temperature.

In this model, a light bulb is switched on during the hours when it is dark outside and people are awake. We determine the ambient light level from the National Renewable Energy Laboratory's (NREL) solar irradiation data at the system location - Jamshedpur, India [11]. The interviews conducted during a field trial were used to assess when people are awake and when they are likely to use indoor or outdoor light bulbs. These two time intervals were overlapped to determine the amount of hours light bulbs are likely to be switched on during each day of a year. The load profile of the fan is modelled on user behavioral information and outside temperature data. The fan is switched on when the outside temperature is high (more than 31°C). Cellphone usage is harder to accurately predict as it is strongly dependent on the number of phones per household. During the interviews, it was confirmed that the number of phones per household varies and is dependent on the number of people in the house. In the model, an average of one phone per household is charged every day. The time the phone starts charging can vary, however, the phone is usually charged for at least three hours per day.

The load profile generated by the usage model is a plot of the output power as a function of time. From this plot in the time domain, the histogram of the fraction of time the system spends at each power level is calculated. The percentage of energy processed by the load converter at each power level is then derived from the time histogram, as shown in Fig. 7.

B. Weighted Efficiency

A power converter's efficiency curve is a fundamental indicator of its performance. Many well-known efficiency metrics are derived from the efficiency curve, for example, the California Energy Commission (CEC) efficiency is a weighted average of the efficiencies at six power levels

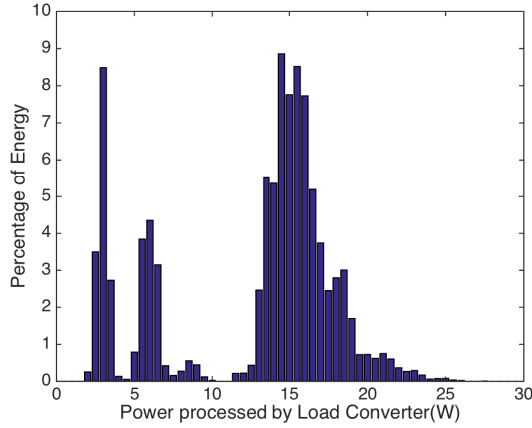


Figure 7: Percentage of energy processed by the load converter including variation in each load's power consumption

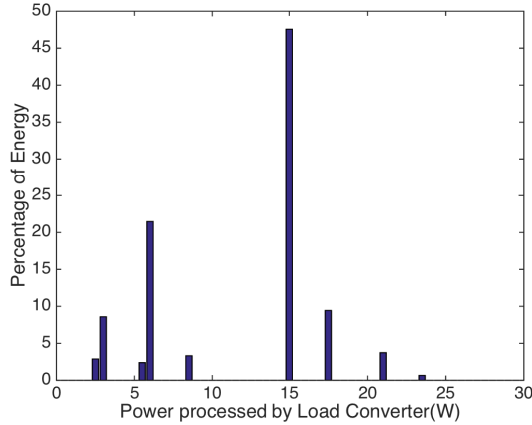


Figure 8: Percentage of energy processed by the load converter, assuming no variation in each load's power consumption

($\eta_{CEC} = 0.04\eta_{10\%} + 0.05\eta_{20\%} + 0.12\eta_{30\%} + 0.21\eta_{50\%} + 0.53\eta_{75\%} + 0.05\eta_{100\%}$). The CEC efficiency gives more weight to the efficiency at high loads, however, the load profiles of many power applications, including the rural electrification microgrid considered in this paper, are dominated by light-load and mid-load usage. Therefore, given the knowledge of the system's load profile, an efficiency metric that reflects the converter's performance in the system more effectively can be derived. By removing load variation (e.g. an LED light consuming 3.1 W is considered to be consuming 3 W) and aggregating consecutive power level bins with low percentages of energy output, we obtain a consolidated version of the percentage of energy processed by the load converter at each power level, as shown in Fig. 8. This gives us the weighted energy metric, as in Equation. 1. Using this metric, the weighted efficiency of the three converters is calculated, as shown in Table. IV.

$$\eta_{energy} = 0.11\eta_{12\%} + 0.24\eta_{24\%} + 0.03\eta_{34\%} + 0.48\eta_{60\%} + 0.09\eta_{70\%} + 0.04\eta_{84\%} + 0.01\eta_{94\%} \quad (1)$$

Table IV: Weighted efficiency metric for three converters

Converter	η_{energy}
Flyback	85.82%
Resonant (Litz wire)	93.17%
Resonant (PCB)	91.96%

V. DETERMINING THE COST OF POWER CONVERTER'S EFFICIENCY

A more efficient power converter may require a more complex topology and higher cost of production. Despite saving some cost by reducing power loss in the system, an overly complicated converter may cost more than the total amount it can save over the system lifetime. To calculate whether the increase in efficiency of the converter justifies the increase in cost, a system-level simulation is performed. For each converter topology under consideration, we first calculate the corresponding optimal solar panel and battery capacities, then calculate the related initial cost and lifetime cost of the system. The initial cost sums up the cost of all components, while the lifetime cost accounts for the cost of replacement of components during the lifetime.

The following subsections describe the steps required to calculate the total system cost. These steps are summarized in the flowchart in Fig. 9.

1) *Set Availability Preference*: Regardless of the choice of load converter topology, the system should be able to provide similar amount of energy. Specifically we define the system availability as the ratio of energy provided to energy demand. Therefore, the system parameters, such as the size of PV panel and battery, must be configured such that the minimum availability level is met. Because the three load converter prototypes have different efficiency characteristics, the corresponding optimal system configurations that yield similar availability level can be different. Given a load converter and its efficiency curve, we iterate through the sizing of PV panel and battery until the system reaches the desired availability. Note that the system cost increases greatly as the availability preference is increased higher than 90%, because high availability level requires electricity provision even in a very rare case. Hence, the cost of providing 100% availability is much higher than the cost of non-served energy. An availability of 92% is chosen for the simulation.

2) *Calculate Generation and Load Profiles*: The generation profile is derived from solar irradiance data of the target location - Jamshedpur, India. The power generated by the solar panels is calculated throughout a year from the annual irradiance data from NREL and the capacity of those panels. The resulting generation profile is a plot of the power generated as a function of time. Similarly, the load profile is determined

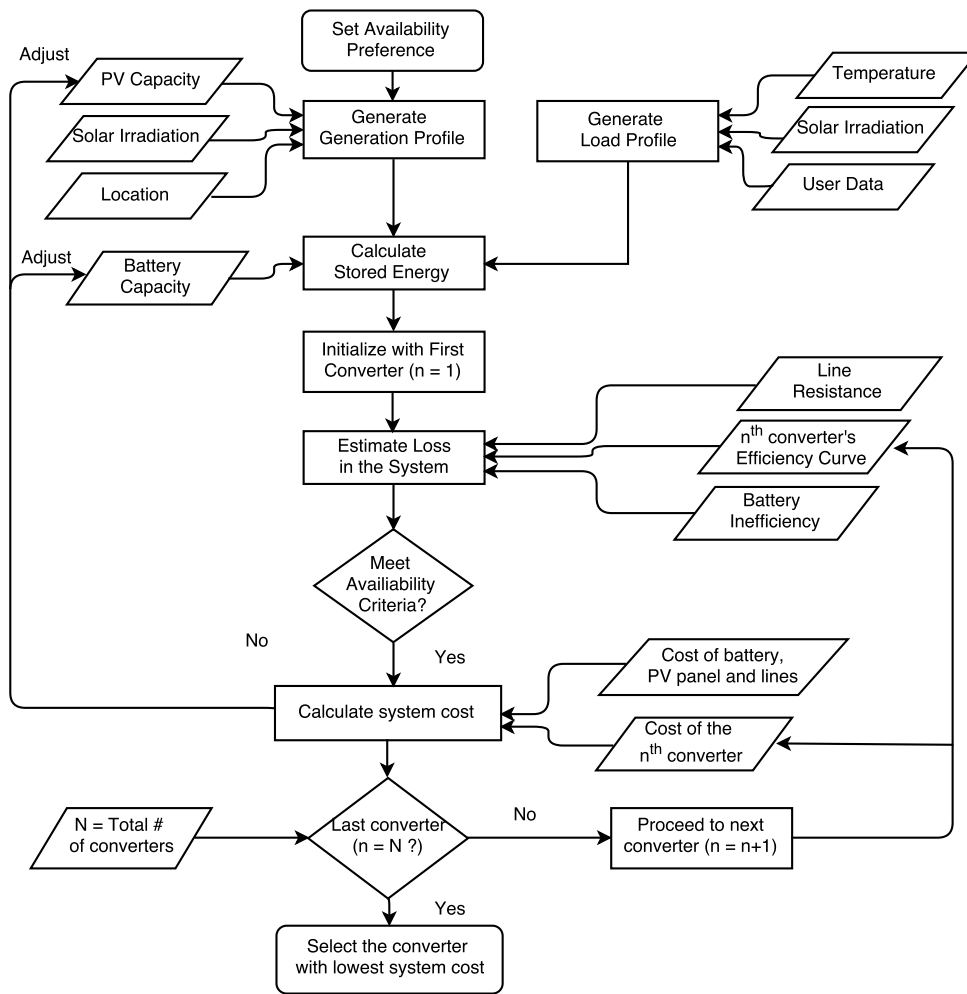


Figure 9: Flowchart showing the steps to determine system cost for each power converter

from user behavioral model and various system characteristics, as discussed earlier in Section IV-A.

3) *Stored Energy*: The difference between power generated and output power is the amount available for storage in the battery. The amount of energy stored in the system also depends greatly on the battery capacity. If the battery is already fully charged, any extra power generated will not be stored, resulting in “spillage”. Therefore, if the battery is too small, the system can not fully utilize the capability of solar energy source and may fail to provide enough output energy to meet the availability requirement. On the contrary, if the battery is too large, it will significantly increase the system cost. This sizing problem presents the trade-off between the battery cost and the availability level.

4) *Losses in the System*: System losses affect the sizing of power generation and required storage necessary to meet the availability requirement. A system with higher power loss from source to load will need a larger power source and storage to provide the same output power as a system with lesser loss.

As illustrated in Fig. 1, the system loss consists of converter inefficiency, battery charging/discharging inefficiency, and line resistances. By tracking the power flow between different points throughout the system, the losses can be calculated.

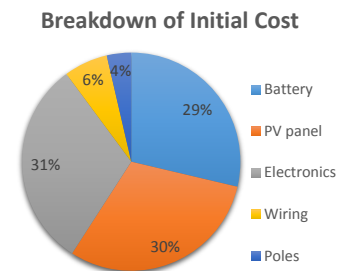


Figure 10: Cost breakdown of the system with five Flyback load converters and one source converter

Table V: Initial and lifetime cost of the system for 92% availability

Converter	Battery Capacity	PV Panel Capacity	Power Stage (\$/unit)	Power Stage (\$/5 units)	Initial System (\$)	Lifetime System Cost
Flyback	22 Ah	200 W	\$5.28	\$26.4	\$460	\$757.4
Resonant (litz wire)	20 Ah	180 W	\$12.54	\$62.7	\$470.4	\$743.7
Resonant (PCB)	20 Ah	190 W	\$8.85	\$44.3	\$458.9	\$732.2

Table VI: System parameters and cost of components used

Parameters	Value
System Parameters	
Number of source units	1
Number of load units	5
Number of Poles	5
Wiring length (per household) from source	40 m
Wiring size	2.55 mm ²
Network voltage	24 V
Availability	92 %
Battery (LFP) lifetime	5 years
Pole (bamboo) lifetime	5 year
System lifetime	15 years
Cost	
PV panel	\$0.7/W
LFP battery	\$0.5/Wh
Power wire	\$0.06/m
Cat3 cable	\$0.03/m
Poles (bamboo)	\$3.33/pole
Source Unit	\$40
Load Unit	\$15 + power stage cost

5) *Iterating and Comparing System Costs*: The system's initial cost includes the cost of PV panel, battery, source and load converters, distribution lines, and mounting poles, as summarized in Table VI. The lifetime cost, over 15 years in this case, includes the additional replacement cost for system components. The battery (Lithium Ferro Phosphate) and the bamboo poles must be replaced every 5 years. The simulation is designed to produce the optimal configuration of PV panels and batteries resulting in the lowest lifetime cost. Because the system's energy availability is a function of the PV panel capacity, battery capacity, as well as the loss incurred, we must find the range of system specifications that can meet the target availability for each load converter. For a given converter, we iterate through different combinations of PV panel capacity and battery capacity, repeat the loss calculation, and compare the resulting availability with the target value. The configurations that meet the availability criteria proceed to the next step of system cost calculation.

Fig. 10 provides a breakdown of the initial capital cost of the system with flyback converter. The simulation process is repeated for the three power converters in consideration. The converter with lowest lifetime cost is then selected. Table V summarizes the results of the simulation. The resonant power converter with PCB transformer, despite having higher production cost than the flyback converter, leads to an optimal system with improved initial *and* lifetime costs. The decrease in initial system cost is due to the converter's lower cost and higher weighted efficiency, which reduces the initial sizing - and hence cost - of other system components. The improved

lifetime cost of the system also follows from this advantage, specifically the lower battery capacity which needs to be replaced after every five years.

VI. CONCLUSION AND FUTURE WORK

This paper presents a methodology to co-design and co-optimize power converters with a new power system. The proposed methodology is demonstrated through an analysis of a rural electrification microgrid design. To minimize the system's lifetime cost, we develop an approach to evaluate and compare the cost effectiveness of implementing different load converters. First, a model is created to estimate the annual load profile. A weighted efficiency metric is then derived from the model to evaluate the load converter. Combining the new efficiency metric definition and a converter's efficiency versus output power curve yields the weighted efficiency value for the converter in context of the system. This metric can indicate a converter choice that minimizes energy loss at the load side, which often translates to smaller sizing for PV panel and storage but does not guarantee the minimum initial or lifetime cost for the system. For each load converter, we run a system-level simulation to find the range of corresponding system configurations that meet the required specification. From these configurations, we select the one that has the lowest lifetime cost for the system. Lastly, the most optimal configuration for each type of converter is compared with the others to find the best possible option for the system.

The analysis in this work considers only load converter's 12 V main power stage. This can be extended to also include other converters and multiple outputs of the converter.

REFERENCES

- [1] C. Sullivan, "Cost-constrained selection of strand diameter and number in a litz-wire transformer winding," *Power Electronics, IEEE Transactions on*, vol. 16, pp. 281–288, Mar 2001.
- [2] B. Burger, D. Kranzer, and O. Stalter, "Cost reduction of pv-inverters with sic-dmosfets," in *Integrated Power Systems (CIPS), 2008 5th International Conference on*, pp. 1–5, March 2008.
- [3] K. Ma and F. Blaabjerg, "Reliability-cost models for the power switching devices of wind power converters," in *Power Electronics for Distributed Generation Systems (PEDG), 2012 3rd IEEE International Symposium on*, pp. 820–827, June 2012.
- [4] X. Yu and A. Khambadkone, "Reliability analysis and cost optimization of parallel-inverter system," *Industrial Electronics, IEEE Transactions on*, vol. 59, pp. 3881–3889, Oct 2012.
- [5] K. Kim, S. Lertburapa, C. Xu, and P. Krein, "Efficiency and cost trade-offs for designing module integrated converter photovoltaic systems," in *Power and Energy Conference at Illinois (PECI), 2012 IEEE*, pp. 1–7, Feb 2012.
- [6] R. Burkart and J. Kolar, "Component cost models for multi-objective optimizations of switched-mode power converters," in *Energy Conversion Congress and Exposition (ECCE), 2013 IEEE*, pp. 2139–2146, Sept 2013.

- [7] C. Calwell, S. Foster, T. Reeder, and A. Mansoor, "Test method for calculating the energy efficiency of single-voltage external ac-dc and ac-ac power supplies," *Energy Star® Adapter Test Methodology*, 2004.
- [8] IEA, *World Energy Outlook 2015*. International Energy Agency, 2015.
- [9] W. Inam, D. Strawser, K. Afridi, R. Ram, and D. Perreault, "Architecture and system analysis of microgrids with peer-to-peer electricity sharing to create a marketplace which enables energy access," in *Power Electronics and ECCE Asia (ICPE-ECCE Asia), 2015 9th International Conference on*, pp. 464–469, June 2015.
- [10] R. W. Erickson and D. Maksimovic, "A multiple-winding magnetics model having directly measurable parameters," in *Power Electronics Specialists Conference, 1998. PESC 98 Record. 29th Annual IEEE, vol. 2*, pp. 1472–1478 vol.2, May 1998.
- [11] "National solar radiation database (nsrdb)."